

# EFFECTS OF GEOMETRY ASPECTS ON THE SIMULATION OF SUPERPLASTICITY IN MMC COMPOSITES

**A. Abedian, A. Barakati, A. Malekpour**  
**Department of Aerospace Engineering,**  
**Sharif University of Technology, Tehran, Iran**

**Keywords:** *Superplasticity, Finite Element Method, Metal Matrix Composite*

## Abstract

*In aerospace applications, the weight of structures is considered as a major performance parameter. One of the most effective ways for weight reduction is superplastic forming. By this technique, not only the weight, but also the stress concentration, the cost, and the time of manufacturing are noticeably reduced. Additionally, the components with complicated shapes could be formed in a single manufacturing step. Due to the wide demand for whiskers reinforced metal matrix composites (MMC's) in aerospace applications, many research works have been designed to extend the borders of superplastic forming of metals to the area of MMC manufacturing. In the present study, the FEM modeling of superplasticity in MMC's is simulated with a micromechanical axisymmetric model. The results are in a good agreement with available experimental data. Various aspects have been considered to show the capabilities of the model to analysis and predict the superplastic behavior of MMC's.*

## 1 Introduction

The magic of superplasticity in conforming materials to complicated shapes is the opportunity that the advantages are taken by many manufacturers. Namely, the monolithic characteristic of the parts made using the superplasticity phenomenon reduces or omits the further manufacturing costs (like subsequent machining) and the need for parts connectors or fasteners. Also, any strength reduction or

creation of stress concentration fields due to discontinuities is disappeared. Additionally, it causes a considerable weight reduction which is the most important issue for the aerospace industry. Notably, with this manufacturing technique, materials with poor formability characteristics (like whisker reinforced metal matrix composites e.g.  $Al/SiC_w$ ) are conformed to complicated shapes.

In some materials due to possibility of promoting the stress flow, the phenomenon of superplasticity is observed. In such occasions, in crystalline materials, elongations of up to several hundred percentages or higher could happen without any trace of irregular or sharp changes in the cross section. In fact, the stress flow is highly dependent on the rate of plastic strain in the material. When this relationship happens to be linear, the conditions of Newtonian viscous flow will persist, i.e. the material will behave like glass, where it can go through a very large deformation without any sign of necking in the sample. This is best explained considering the Backofen equation [1];

$$\dot{\epsilon} = A\sigma^n \quad (1)$$

$$\text{or } \sigma = B\dot{\epsilon}^m \text{ where } m = 1/n$$

For  $n=1$  (or  $m=1$ , the strain rate sensitivity) the relationship between  $\dot{\epsilon}$  and  $\sigma$  will be linear. For a simple tension test, the following equation can be derived;

$$\sigma = \frac{P}{A} = B\dot{\epsilon}^m \rightarrow A = \frac{P}{B}\dot{\epsilon}^{-m} \quad (2)$$

where  $P$  is the tensile load and  $A$  is the cross section of the sample. Taking the time derivative of Equation (2) yields;

$$-\frac{dA}{dt} = \frac{P}{B} \dot{\epsilon}^{-m+1} = \frac{P/m}{B} \frac{1}{A^{(1-m)/m}} \quad (3)$$

This derivation means that for  $m = 1$ , the rate of change in cross section of the sample is independent of the area of the cross section, or in other words, the carried load is independent of the area “ $A$ ”. With increasing  $m$  to one, the superplastic conformation of the material will occur with less and less necking.

So far, many researchers have performed a number of experiments to explain the deformation mechanisms and also to optimize the process [2-5]. Two of the well known mechanisms distinguished by these research studies are referred to as the Fine Structure Superplasticity (FSS) and the Internal Stress Superplasticity (ISS). The former applies to the materials with fine grain structures, where the strain rate sensitivity is around 0.5 and the plastic deformation occurs by means of the grain-boundary sliding mechanism. While, the latter applies to either the materials which go through a phase change under thermal cycling (like *Ni-Fe* alloys), or the materials which possess different coefficients of thermal expansion (CTE’s) in different directions (like *Zinc* and  $\alpha$ -*Uranium*) or include phases with different CTE’s (like *Al/SiC* composites). Note that for the ISS regime, since the plasticity occurs by means of slip deformation mechanism and the strain rate sensitivity is close to one, the size of grain is not of great importance.

Two different practical approaches distinguished based on the kind of loading, i.e. isothermal and thermal cycling, are employed for imposing superplastic deformation by the ISS mechanism. For the first approach, which is more common in practice, the forming is performed in a constant temperature. In this method, the strain rate is relatively high. However, for the second method, which is so called thermal cycling superplasticity, the strain rate is low and in average it falls in the range of  $10^{-5} - 10^{-4} s^{-1}$ . Note that in general, the thermal

cycling approach creates higher elongations compared to the isothermal approach [2, 4].

The thermal cycling approach along with an external tensile mechanical stress, which is also considered to be small and constant, is employed for superplastic forming of metal matrix composites reinforced with ceramic whiskers. Note that these materials have found much interest in the aerospace industry due to their superior properties. Here, the difference in CTE’s of the fiber and matrix creates large interfacial internal stresses which depending on the characteristics of the applied thermal cycle they could increase to the values higher than the yield strength of the matrix causing plastic deformation in the composite. However, since in this approach a thermal cycling regime is applied, the plastic strain is totally vanishes when the temperature is reversed in the next half cycle. Here, the applied small mechanical stress biases the stress field generated during the thermal cycle, causing a small permanent plastic strain, which with repeating the thermal cycle, it starts to accumulate [6,7]. This has been developed into a more soundly based quantitative predictive model using the Lavy-von Mises flow rules and has been further developed for other cases of the phenomenon [8], where more details could also be found in [9].

Keeping in mind the complication involved, to understand the deformation mechanisms and the interrelationship between the constituents of the composites in the event of superplastic behavior, it is necessary to analyze the problem carefully. However, as the experimental works are time consuming, costly, and very equipment dependent, analytical and numerical tools, which have not widely been considered, must be developed. Since the analytical studies involve with very complicated PDE’s that require so many assumptions to become solvable, numerical methods such as the Finite Element Method (FEM) may ease the solution. Although very careful geometry and material modeling, as well as the meshing, and employing nonlinear procedures (such as stepping and updating the stiffness matrix in each step) are necessary. It should be mentioned

that due to the complications involved only a few FEM studies would be found in the literature [10-14].

In the most recent FEM study [9], assuming a regular distribution for the whiskers, an axisymmetric micromechanical model has been used for modeling the behavior of  $Al/SiC_w$  composite under superplastic loading conditions. Although the study showed that the modeling is fundamentally acceptable, there is still a long way for generalization of the approach. For example, due to some differences that were detected between the experimental data and the calculated FEM results [15], the model seems to need some modifications.

The present study offers a new image of the published results and also tries to discuss some of the subjects in more details from a different angle. Specifically, the data collection is done in a different way here. In contrary to the previous work, instead of collecting the data from some points in the matrix region, it is done in an average manner. Also, the necking phenomenon in the larger applied mechanical loads is analyzed both using the local and average data collection approaches. The effects of fiber volume fraction, fiber/matrix debonding, and matrix hardening characteristics are discussed, as well.

## 2 Material, Loading and Geometry Modeling

Modeling of all aspects of the geometry, materials, and loading will definitely produce more precise and reliable outputs. However, for reducing the cost of calculations and overcoming the hardware and software limitations, it is necessary to adopt some simplification assumptions regarding the geometry modeling. The SEM photos of the cross-section of MMC's have shown that the added  $SiC_w$  to the aluminum matrix are dispersed in the direction of extrusion axis [16]. Also, the photos show that the misalignment of about 30% of the whiskers is limited to  $\pm 9.3^\circ$  while the rest are more or less aligned [17]. Therefore, it could be assumed that the fibers are of circular cross-section and aligned as

shown in Fig. 1 (a). Such an assumption makes it possible to simulate the whole composite with an axisymmetric micromechanical model, see Fig. 1 (b). The applied boundary conditions are presented in Fig. 1 (c). The history of the introduced model goes back to the simulation attempts for predicting creep behavior of a similar composite, where it provided very satisfactory results [15].

Since the fiber/matrix debonding is an important factor in controlling the composite deformation, as it has been the case for predicting creep behavior of MMC's [18], this phenomenon is considered in this study, as well. Fig. 2 shows different states of debonding at the fiber/matrix interface that are considered in this study. It should be noted that for the case of creep simulation it was found that  $0 \leq \zeta \leq 0.5$  is meaningful, where for  $\zeta = 0.5$  half of a fiber length is considered to be debonded. Above this value, not any sign of fiber effects could be distinguished, i.e. the matrix creeps as if no fiber presents in the unit. A full explanation of the debonding phenomenon could be found in [15]. But for the subject under consideration, no limiting border for  $\zeta$  is set, yet. Therefore, selecting  $0 \leq \zeta \leq 0.5$  in this study is done, arbitrarily. However, it should be noted that the fiber misalignment, fiber offsetting, and the fiber and unit cell geometric ratios (aspect ratios), which could also affect the rate of deformations are ignored here.

As for the meshing, uniform nonlinear quadrilateral elements were considered. The Plane-82 of ANSYS element library, which is a 2-D axisymmetric nonlinear elasto-viscoplastic element, is used for the geometry meshing. But, it should be noted that an extraordinary stress field is developed at the sharp corner of the fiber, where for computing the effects of this field on the inelastic behavior of the material, it is necessary to place very fine mesh in this region [18]. This effect is also added to the study and the results will be discussed later.

The fiber volume fraction ( $V_f$ ) is calculated as shown by Equation (4);

$$V_f = \left(\frac{r}{b}\right)^3 \frac{AR_f}{AR_u} \quad (4)$$

where  $r$  and  $b$  are the fiber and the unit cell radii, and  $AR_f$  and  $AR_u$  are the fiber and the unit cell aspect ratios, respectively. Here, volume fractions of 10 and 20 percent and  $AR_f = 4$  are considered [16].

In this study it is assumed that the fibers remain elastic during the whole process, while the 2024Al matrix behaves in an elastic perfectly plastic manner. Also, for better understanding of the effects of any strain hardening characteristic of the matrix, a bilinear stress-strain curve with plastic modulus or secant modulus of some values is assumed. A summary of the properties assumed for the fiber and matrix is presented in Table 1.

**Table 1.** Material properties for Al2024/SiC<sub>w</sub> constituents [16]

Material	E [GPa]	CTE [K <sup>-1</sup> ]	$\nu$	$\sigma_y$ [MPa]
2024 Al	73	24.7x10 <sup>-6</sup>	0.33	30
SiC	470	4.6x10 <sup>-6</sup>	0.17	-

As for the loading, according to the literature available on the experimental superplasticity [16], it is assumed that a thermal cycling regime, as in Fig. 3, along with a small constant tensile mechanical stress is applied to the model. For the heating phase of the cycle, the composite is heated between 100°C – 450°C in only 50 seconds, while it is cooled down to 100°C from the maximum of 450°C during 150 seconds [16]. This thermal cycle is accompanied with a constant longitudinal small mechanical stress of magnitude 2, 4, 7, and 10MPa [16] to form the biased stress for promoting superplastic deformation.

### 3 Results and discussion

As mentioned before, for the ISS mechanism, with increasing the number of applied thermal cycle in presence of the mechanical load, the plastic strain starts to accumulate.

Based on the results published in [9], with the linear relationship of the accumulated plastic strain ( $\epsilon_p$ ) with the number of cycles ( $N$ ) for all the constant mechanical load cases considered in that study, one could find the strain rate ( $\dot{\epsilon}$ ) from Equation (5);

$$\dot{\epsilon} = \frac{d\epsilon_p}{dN} \cdot \frac{1}{\tau} \quad (5)$$

where  $d\epsilon$  represents the accumulated plastic strain in a given number of cycles (i.e.  $dN$ ) and  $\tau$  indicates the period of the applied thermal cycle [16]. Then the log-log scale plot of the  $\dot{\epsilon}$  values vs. the applied mechanical load indicated a power law type relationship (as in Equation (1)) for the material behavior. There, the power  $n = 1.8$  was found to be in a good agreement with the experimental results of  $n = 1.6$ . Although, some differences between the calculated and the experimentally measured values of  $\dot{\epsilon}$  were evident.

These valuable results were, however, not valid for every point of the model due to the shortcomings of the data collection procedure used in that study. The data was taken from a node inside the matrix close to the interface region in the neighborhood of the fiber end. Replacing the node with, for example, another node placed at the model end, some great differences in the nature and the values of the strain could be realized. Therefore, the need for a general data collection was clear and also to necessary to develop. This task is fulfilled here with the use of averaging idea put forward by Hsueh in [19] for calculation of the average elastic strain, but with applying some modifications to the proposed procedure. In that study the average values of the nodal and then elemental displacements were used to calculate the average elastic strain. However, since the average plastic strain calculation for the FEM model is of interest here, the average of elemental  $\epsilon_p$  was incorporated into the Equation (6);

$$\bar{\varepsilon}_p = \frac{1}{\pi b^2 L} \sum_{i=1}^n \left[ \int_{z_i}^{z_{2i}} \int_{r_i}^{r_{2i}} 2\pi \bar{\varepsilon}_{p_i} r dr dz \right] \quad (6)$$

where  $\bar{\varepsilon}_p$  represents the average plastic strain over the entire model,  $z_i$  and  $r_i$  represent the  $z$ - and  $r$ -dimensions of the  $i$ th element,  $\bar{\varepsilon}_{p_i}$  is the elemental plastic strain, and  $b$  and  $L$  are the radius and the length of the model, respectively.

Fig. 4 (a) presents the plastic strain vs. the number of cycles (time) for four mechanical loads of 2, 4, 7, and 10 MPa applied to the model. Interestingly, the averaging technique confirms the linear relationship of the  $\varepsilon_p$  vs.  $N$  graphs, which is the fundamental issue for calculating  $\dot{\varepsilon}$  values by the use of Equation (5). Plotting the calculated  $\dot{\varepsilon}$  values vs. the corresponding stresses, one would see the power of  $n$  in Equation (1) drops to 0.56 (see Fig. 4(b)) from  $n=1.8$  for the case of local data collection as in [9].

To check whether these differences are not due to the error that may involve with the averaging technique, the mechanical stress was taken off the model and the response of the material only under the applied thermal cycle was monitored. As it is seen in Fig. 5 (a), for the case of perfect bond with  $V_f = 20\%$ , the plastic strain in heating phase of the cycle is compressive and with cooling the composite, the compressive strain disappears and a tensile strain shows up. Note that the matrix was assumed to be elastic-perfectly plastic. Interestingly, this result shows that the averaging technique leaves no strain residue after so many cycles. Additionally, it was shown that this technique, even in presence imperfections like fiber/matrix debonding, performs perfectly; see Fig. 5 (b). This is clearly shown that for the case of  $\zeta = 0.25\%$  ( $\zeta$  represents the percentage of the fiber length debonded from the matrix) also no strain residue is calculated by the averaging technique.

To see how the averaging technique performs in presence of both fiber/matrix debonding and the mechanical applied stress, the data collected by the local technique was

reproduced here using the averaging technique. As it is seen in Fig. 4 (b), the power  $n$  is shifted back to 1.8 with considering  $\zeta = 0.25$  and the values of  $\dot{\varepsilon}$  are also get closer to the experimental results compared to the case of perfect bond. Note that for the case of local data collection, the debonding was worsening the value of  $n$ , while the  $\dot{\varepsilon}$  values were shifted toward the experimental results, see Fig. 4 (c).

Another interesting result that could promote further enthusiasm to be put into the efforts for further development of the averaging technique is related to the little bent or a small change in the slope of the average line of the graph of  $\varepsilon_p$  vs.  $N$  in the middle of the superplastic process for the case of  $\sigma = 10 \text{ MPa}$  reported in [9], see Fig. 6 (a). Interestingly, the bent or change in slope for the case of  $\sigma = 10 \text{ MPa}$  is also calculated by the averaging technique, see Fig. 6 (b). Note the straight line for the case of  $\sigma = 4 \text{ MPa}$ , although the strain values appear to be different. Therefore, it could be concluded that during the superplastic forming of composites, for higher stress values, another mechanism rather than Newtonian viscous flow may come into effect which may need a special treatment.

This is given a try here by considering some derivation in the assumption of elastic-perfectly plastic behavior for the matrix material. This is considered because during the plastic deformation a kind of hardening or softening due to the material imperfection or impurities may happen that causes the plastic deformation to go out of the regular expected path. Figs.7 (a) and 7 (b) show the plastic strain vs.  $N$  for  $\sigma = 4 \text{ MPa}$  calculated by both the averaging and local data collection techniques, respectively, for the case of some percentages of secant modulus that many brought about some small amount of material hardening. As it is seen, both methods even for small values of applied mechanical stress could detect a change in slope of the average line of the graph of  $\varepsilon_p$  vs.  $N$ . However, note the decay in the amplitude of the plastic deformation. More modeling is under way for finding the basic

reason behind the phenomenon and the ways for avoiding the change in the slope.

**4 Conclusions**

From the study performed here one can highlight the followings:

- 1- The averaging technique introduced here helps the data collection to be done in a more general manner, though more aspects of it should be known and further developed.
- 2- Based on the results found by the averaging technique the FEM model needs some more modifications before it could be successfully used for predicting all the aspects of the superplastic behavior of the MMC composite.
- 3- It is now clear that there should be a kind of close control over the mechanical loading regime in superplastic forming of materials. The high loads may cause some sort of hardening or the material imperfections may inflict some kind of softening that affect the forming by causing necking in the materials samples.
- 4- By the obtained results it is clear that the fiber/matrix debonding should be included in the modeling as an important parameter.

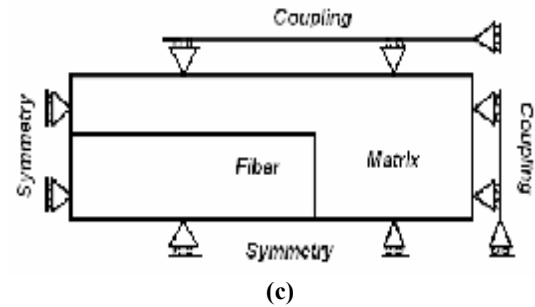
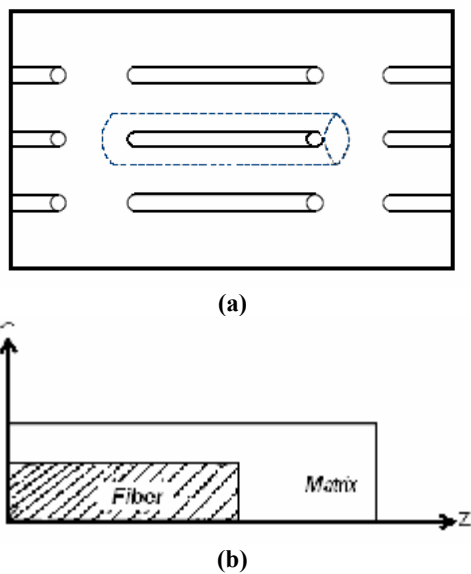


**Fig. 1.** Geometry modeling of the unit, (a) fiber and matrix in a 3-D model, (b) fiber and matrix in a 2-D model, (c) the final modeling of the fiber and matrix and the boundary conditions

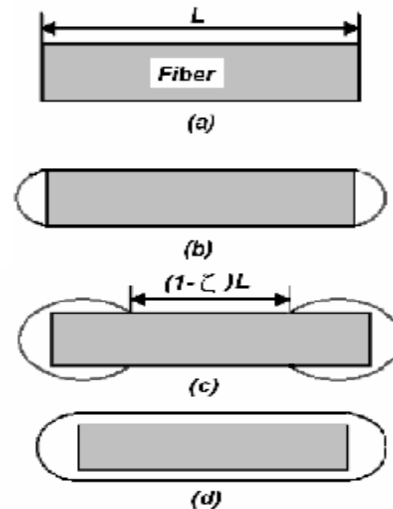


**Fig. 2.** Different situation of debonding at fiber/matrix interface, (a) perfect bond, (b) fiber end debonding, (c) partial debonding, (d) full debonding

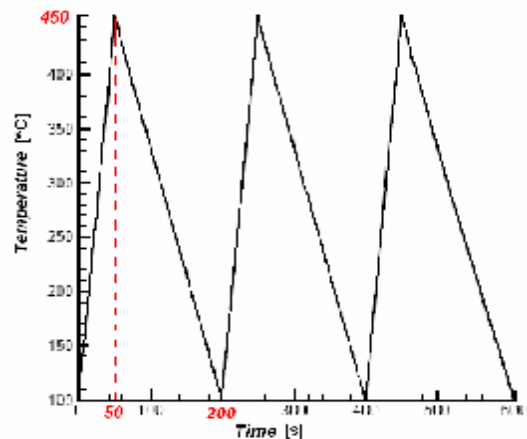
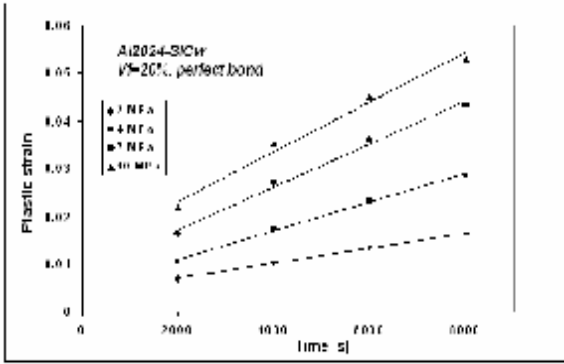
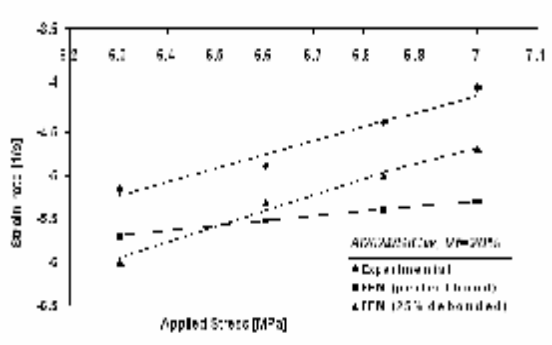


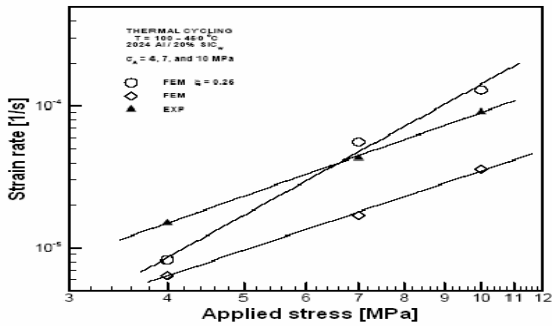
**Fig. 3.** Profile of the applied thermal cycle



(a)

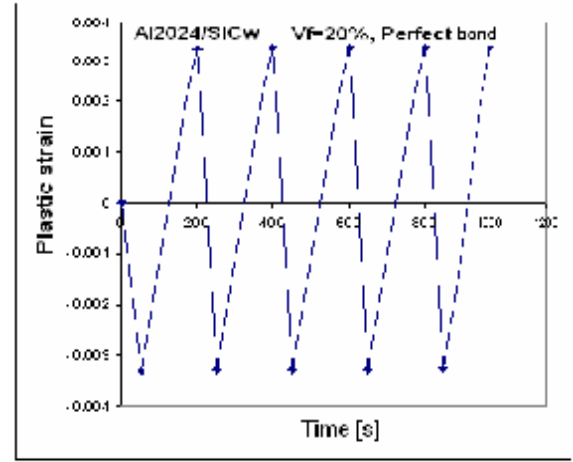


(b)

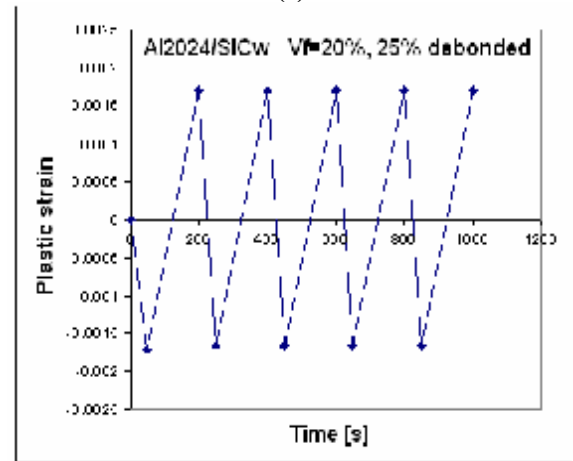


(c)

Fig. 4. FEM results for Al2024/20%SiCw with different applied stress values, (a) plastic strain vs. time, (b)  $\log(\dot{\epsilon})$  vs.  $\log(\sigma)$  with averaging technique, (c)  $\log(\dot{\epsilon})$  vs.  $\log(\sigma)$  with local method

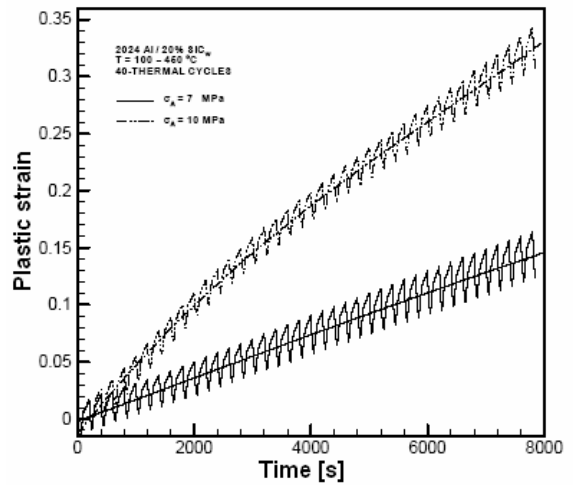


(a)

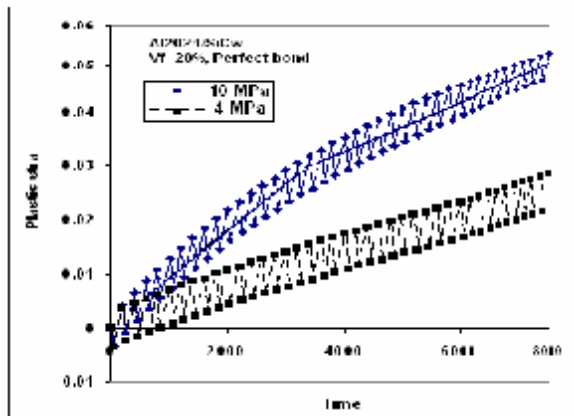


(b)

Fig. 5. FEM results for Al2024/20%SiCw with no applied stresses, (a) with perfect bond, (b) with 25% debonding

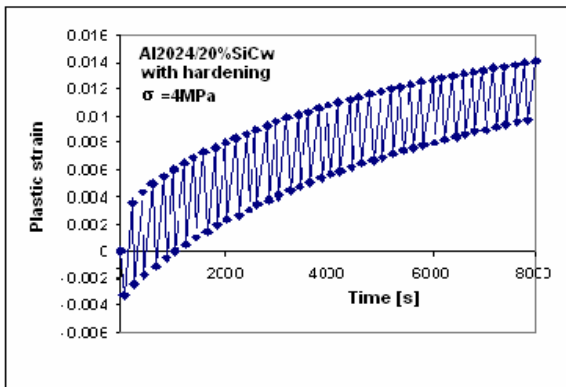


(a)

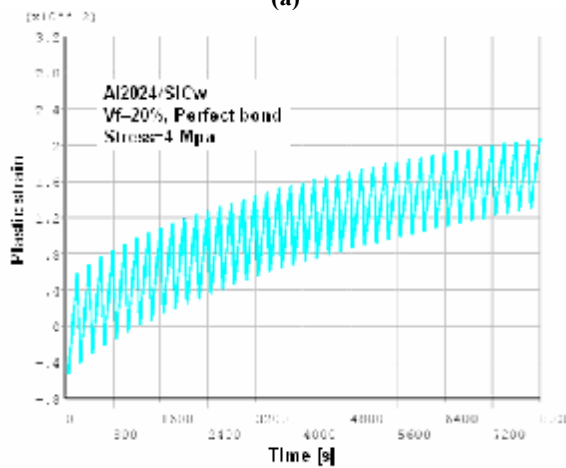


(b)

Fig. 6. Change in the slope of the average line for higher stress values (a) with local data collection, (b) with averaging technique



(a)



(b)

Fig. 7. Considering some values of hardening for the matrix material for  $\sigma = 4 MPa$ , (a) with local data collection, (b) with averaging technique

- [1] Xing H, Wang C, Zhang K and Wang Z. Recent development in the mechanics of superplasticity and its applications. *Journal of Materials Processing Technology*, pp 196-202, 2004.
- [2] Sunder R, Kitazono K, Sato E and Kuribayashi K. Internal stress superplasticity in an in-situ intermetallic matrix composite. *Materials Science Forum*, Orlando, USA, pp 405-410, 2001.
- [3] Han J, Kim M, Joeng H and Yamagata H. High strain rate superplasticity in Al-16Si-5Fe based alloys with and without SiC particles. *Material Forum*, Vols. 357-359, pp 613-618, 2001.
- [4] Nieh T, Wadsworth J and Sherby O. *Superplasticity in metals and ceramics*. Cambridge University Press, 1997.
- [5] Sherby O. Advances in superplasticity and in superplastic materials. *ISIJ International*, Vol. 29, 1989.
- [6] Sosa S and Langdon T. Deformation characteristics of a 3Y-TZP/20%Al<sub>2</sub>O<sub>3</sub> composite in tensile creep. *Material Science Forum*, Vols. 357-359, pp 135-140, 2001.
- [7] Pickard S and Derby B. The deformation of particle reinforced metal matrix composites during temperature cycling. *Acta Metal. Mater.*, vol. 38, No. 12, pp 2537-2552, 1990.
- [8] Derby B, Internal stress superplasticity in metal matrix composites. *Scripta Metall.*, vol. 19, pp 703, 1985.
- [9] Abedian A and Malekpour A. FEM analysis of internal stress superplasticity in Al/SiC<sub>w</sub> composite with different V<sub>F</sub> subjected to thermal cycling. *24<sup>th</sup> ICAS*, 2004.
- [10] Mimaroglu A and Yeinyhat O. Modeling the superplastic deformation process of 2024 aluminum alloys under constant strain rate: use of finite element technique. *Material and Design*, pp 189-195, 2003.
- [11] Zhang H, Daehn G and Wagoner R. Simulation of plastic response of whisker reinforced metal matrix composites under thermal cycling conditions. *Scripta. Metal. Mater.*, Vol. 25, pp. 2285-2290, 1991.
- [12] Zwigl and Dunand D. Transformation-mismatch plasticity of NiAl/ZrO<sub>2</sub> composites-finite element modeling. *Materials Science & Engineering A*, 2002.
- [13] Carrino, Giuliano and Palmieri. On the optimization of superplastic forming processes by the finite element method. *Materials Processing Technology*, pp. 373-377, 2003.
- [14] Yarlaga, Gudimetla and Adam. Finite element analysis of high strain rate superplastic forming (SPF) of Al-Ti alloys. *Material Processing Technology*, 2002.
- [15] Mondali M, Abedian A and Adibnazar A. FEM study of the second stage creep behavior of

References

- Al6061/SiC metal matrix composite. *Computational Material Science*, pp 140-150, 2005.
- [16] Hong S, Sherby O, Divecha A, Karmarker S and MacDonald B. Internal stress superplasticity in 2024Al-SiC whisker reinforced composites, *Journal of Composite Materials*, Vol. 22, pp 102-123, 1988.
- [17] Chan K and Tong G. Strain rate sensitivity of a high-strain-rate superplastic Al606/SiCw composite under uniaxial and equibiaxial tension, *Materials Letters* 51, 2001.
- [18] Abedian A and Mondali M. FEM study of constant rate creep analysis of MMC's, *11th Iranian Annual Conference (International) of Mechanical Engineering*, Vol. 3, pp 1271-1280, 2003.
- [19] Hsueh Chaun-Hway. Young's modulus of unidirectional discontinuous-fiber composites. *Composites Science and Technology*, pp 2671-2680, 2000.